Journal of Structural Geology, Vol. 12, No. 2, pp. 243 to 257, 1990
Printed in Great Britain

0191-8141/90 $03.00+0.00

The kinematic and geodynamic significance of the Atacama fault zone, northern Chile

EKKEHARD SCHEUBER

Institut für Geologie, Freie Universität Berlin, Altensteinstrasse 34 A, D-1000 Berlin 33, F.R.G.

and

PAUL A. M. ANDRIESSEN

Z.W.O. Laboratorium voor Isotopen-Geologie, De Boelelaan 1085, NL-1081 HV Amsterdam, The Netherlands

(*Received* 5 *December* 1988; *accepted in revised form* 13 *June* 1989)

Abstract—The Atacama fault zone (AFZ) is the dominant feature in the structure of the North Chilean Coastal Cordillera. Left lateral displacement took place along its system of longitudinal faults during the Jurassic and early Cretaceous. This development was contemporaneous with arc magmatism and was later reactivated, resulting in a steep normal fault. Strike-slip movements along the AFZ consist of two sets of ductile shear zones of different ages: one Jurassic, formed under amphibolite-facies conditions; the other early Cretaceous, with greenschist-facies mylonites. Structural asymmetries point to a sinistral sense of shear in both sets. The AFZ can be interpreted as a magmatic arc structure which accommodated the oblique subduction of an oceanic plate (trench-linked strike-slip fault). The sinistral sense of shear is consistent with reconstructions of late Jurassic to early Cretaceous plate configurations in the SE Pacific.

INTRODUCTION

SUBDUCTION at an active continental margin, associated with the Andean Cycle (Coira *et al.* 1982), has played a major role in the structural and magmatic evolution of the Central Andes since the beginning of the Jurassic Period. The greatest amount of deformation in a system of converging plates of this kind is probably accommodated in the subduction zone, i.e. in the shear zone between the two plates. Due to the forces generated by plate convergence, the crust of the upper plate may also be deformed. The magmatic arc is one realm that may suffer very strong tectonic deformation, including crustal shortening and/or longitudinal wrenching contemporaneously with plutonism and volcanism (Reutter *et al.* 1988, Reutter & Scheuber 1988). The eastward shift of the magmatic arc towards the interior of the continent during the Andean Cycle resulted in four arc stages (Reutter & Scheuber 1988) (for location see Fig. 1): (1) a Jurassic–early Cretaceous arc in the Coastal Cordillera; (2) a mid-Cretaceous arc in the Longitudinal Valley; (3) a late Cretaceous–Paleogene arc in the Chilean Precordillera (Sierra de Moreno, Cordillera Domeyko); and (4) the Miocene–Holocene arc in the Western Cordillera, with extensions of magmatic activity reaching into the Eastern Cordillera. This paper concentrates on the tectonics of the Jurassic–early Cretaceous magmatic arc of the Coastal Cordillera, of which the Atacama fault zone (AFZ) is a major element. Structures of the AFZ have been investigated and mapped in detail between 24°36′ and 24°56′S (Figs. 2 and 3). Other occurrences of sheared rocks between Antofagasta and Paposo (23°30′–25°S, Fig. 4) and in the Quebrada Chañaral south of Vallenar (≈29°S) have also been taken into consideration (Fig. 1).

GEOLOGICAL SETTING

The Coastal Cordillera is the realm of the Jurassic–early Cretaceous magmatic arc, and it is composed mainly of andesitic tuffs and lavas some 10 km thick (forming the La Negra Formation, Garcia 1967) and of large batholiths of mainly dioritic composition. In the area studied, the volcanic rocks overlie a sequence of late Paleozoic to early Jurassic (Hettangian–Middle Sinemurian) deposits. Continental clastic rocks and marine limestones (Hauterivian–Barremian) recording the end of arc volcanism overlie the Jurassic to early Cretaceous andesites south of Antofagasta. Marine intercalations in the Jurassic volcanic rocks indicate a depositional environment more or less at sea level (Gröschke *et al.* 1988). The extrusion of these thick volcanic rocks was therefore probably accompanied by considerable crustal subsidence. Furthermore, radiometric age determinations (≈200–120 Ma; Halpern 1978, Berg & Breitkreuz 1983, Diaz *et al.* 1985, Hervé *et al.* 1985, Damm *et al.* 1986, Hervé 1987b, and others) showed that huge batholiths intruded during the volcanic regime. The plutonism was initially dioritic to gabbroic, becoming more tonalitic to granodioritic in the younger stages. Initial ratios of Sr-isotopes of Meso-

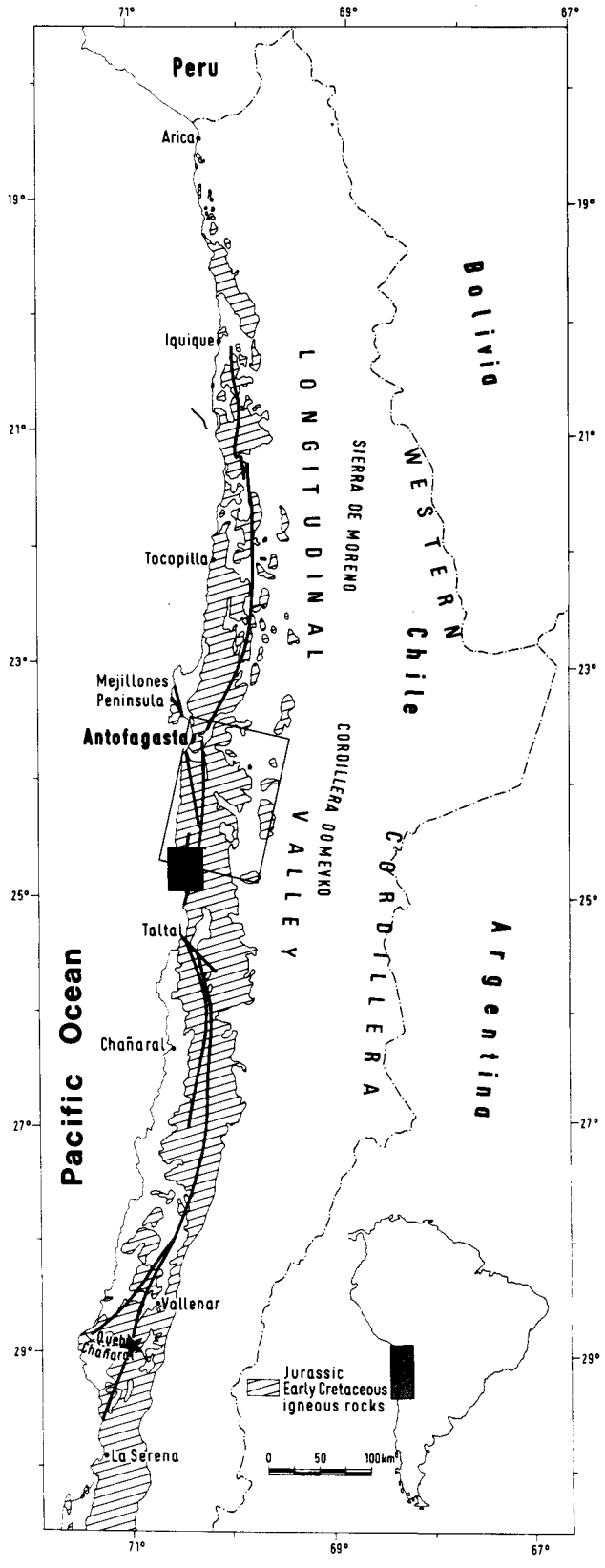

Fig. 1. Map showing the Atacama fault zone (heavy lines) and the distribution of Jurassic to early Cretaceous igneous rocks in the Coastal Cordillera of northern Chile. The black rectangle shows the location of the map of Fig. 2; the rectangular frame shows the location of the satellite image of Fig. 5; the star shows the location of mylonitic rocks in the Quebrada Chañaral (source: Mapa Geológico de Chile 1 : 1,000,000, 1982).

zoic plutonic rocks of the North Chilean Coastal Cordillera fall between 0.713 and 0.703, indicating a mainly subcrustal source for the magmas (McNutt *et al.* 1975, Halpern 1978, Damm & Pichowiak 1981, Berg & Breitkreuz 1983, Diaz *et al.* 1985). The chemical composition of the Jurassic–early Cretaceous plutonic rocks closely resembles that of the calc-alkaline volcanic rocks of the same age (Damm *et al.* 1986), which leads to the conclusion that they are the hypabyssal equivalents of the volcanic rocks.

The Coastal Cordillera as it is today occupies a forearc position and it is characterized structurally by nearly vertical faults that separate blocks exposing different structural levels. Vertical displacements along these faults may be of some significance. One example is the WNW–ESE-trending El Way fault system south of Antofagasta (Fig. 4) which separates a non-metamorphic sequence composed of about 10 km of Jurassic volcanic rocks, 2 km of early Cretaceous conglomerates and 0.5 km of early Cretaceous limestones (Hauterivian–Barremian) to the north from Jurassic gabbros and diorites, partly deformed under amphibolite-facies conditions in Jurassic times, to the south (Rössling 1987). Post-Jurassic vertical displacement along the El Way Fault thus exceeds 12.5 km.

K–Ar and fission-track analyses were performed on several minerals of an amphibolite derived from a Jurassic diorite, located south of Antofagasta (Table 1, Fig. 4). Except for the K–Ar hornblende age of 163 ± 14 Ma, the mineral ages of between 138 and 118 Ma are, within the error range, practically the same. Thus, the major part of the crustal uplift and the subsequent cooling in the Coastal Cordillera had already taken place during the latest Jurassic and the early Cretaceous. Due to this uplift, plutonic rocks, gneisses and amphibolites are exposed over a large area. In older literature, the metamorphic rocks were attributed to the Precambrian–early Paleozoic basement. Recent studies, however, have shown that most of them developed during a Jurassic to early Cretaceous shear deformation from igneous rocks of the same age (Uribe & Niemeyer 1984, Diaz *et al.* 1985, Rössling *et al.* 1986, Scheuber 1987). Amphibolites and mica schists from the northern and middle part of the Mejillones Peninsula (Fig. 4) are the only elements that belong to an older metamorphic basement (probably Cambrian, Damm *et al.* 1986, Diaz *et al.* 1985).

THE ATACAMA FAULT ZONE (AFZ)

The most important fault system in the Coastal Cordillera is the AFZ, a N–S-trending set of faults consisting of several parallel branches that can be followed for more than 1000 km over an area stretching from Iquique (20°30′S) to north of La Serena (29°45′S). Figure 1 shows the AFZ and its close link to Jurassic–early Cretaceous igneous rocks. St. Amand & Allen (1960) postulated a recent dextral strike-slip movement of some 450 km along the AFZ. Arabasz (1971) assumed

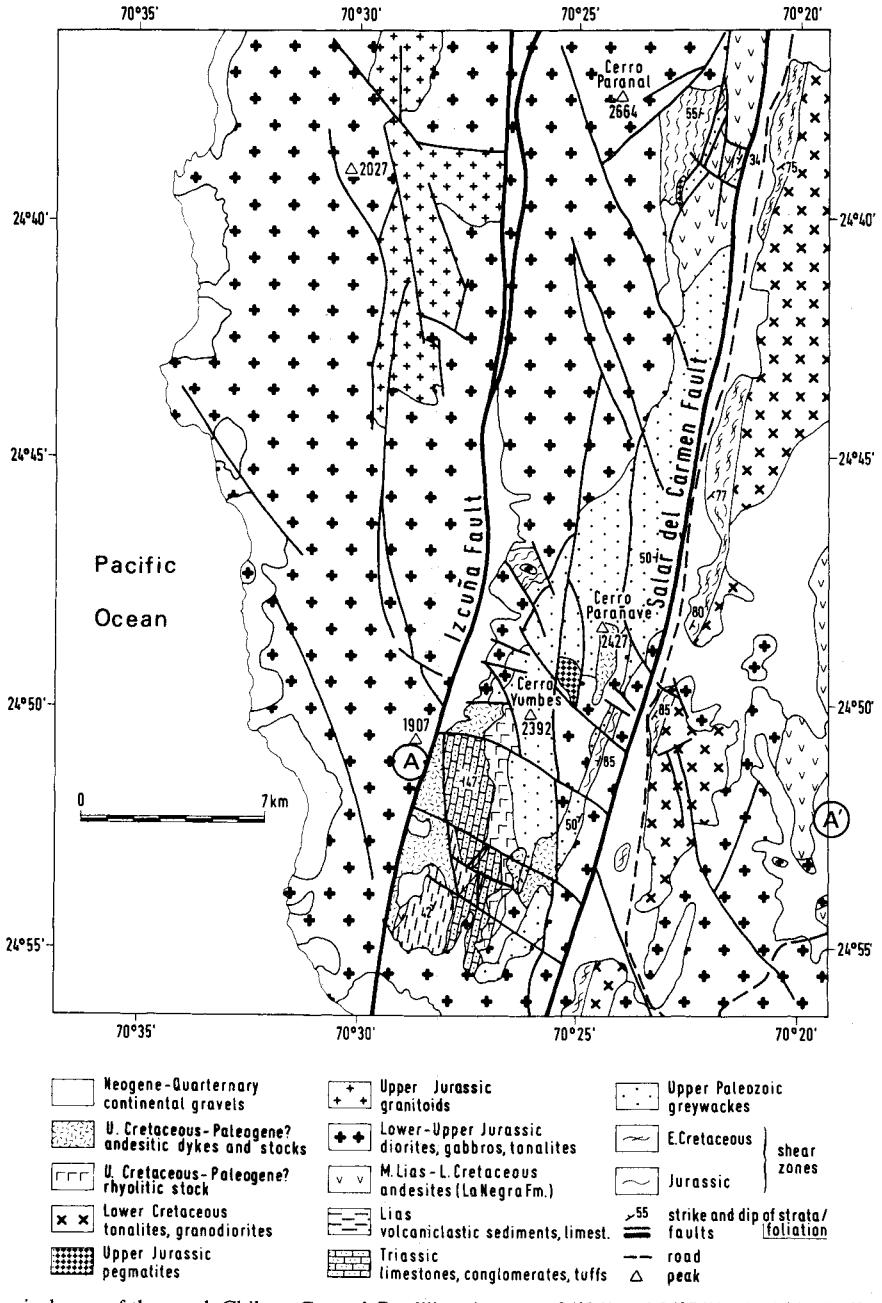

Fig. 2. Geological map of the north Chilean Coastal Cordillera between 24°36′ and 24°56′S, A–A′ is the line of section of Fig. 3 (for location see Figs. 1 and 4).

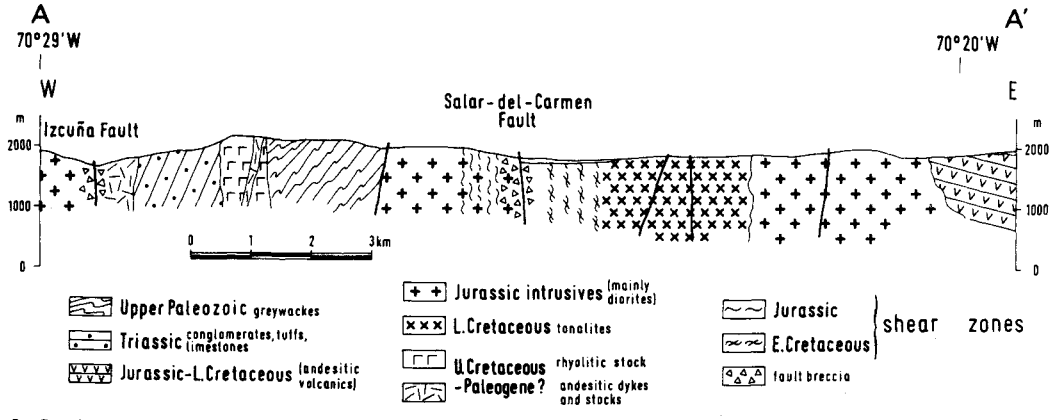

Fig. 3. Section across the Coastal Cordillera at 24°51′S. Section A–A′ is indicated in Fig. 2. The scale of the profile is not identical to that of Fig. 2.

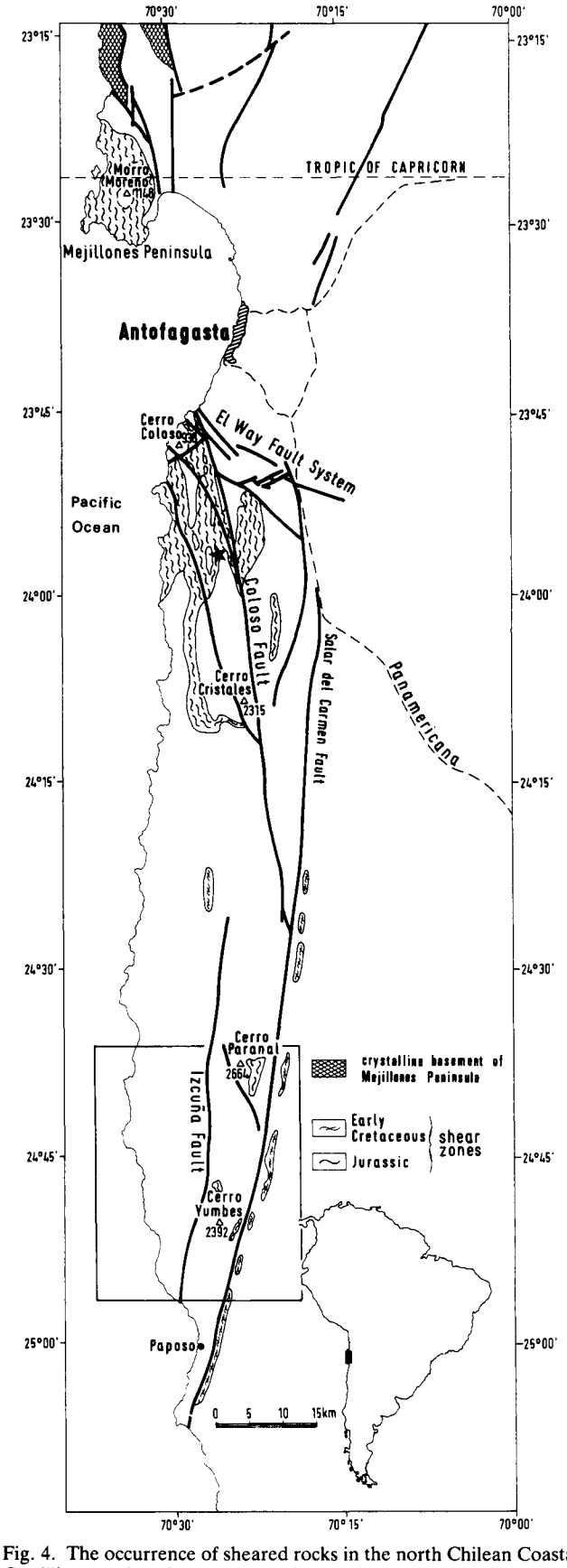

Fig. 4. The occurrence of sheared rocks in the north Chilean Coastal Cordillera north and south of Antofagasta (source: Uribe & Niemeyer 1984, Hervé 1987b, Scheuber 1987 and Rössling 1988); the area of the map of Fig. 2 is indicated by the frame; the star at 23°56'S/70°25'W shows the location of the sample for which fission-track and K–Ar datings are listed in Table. 1. The faults are shown by heavy lines.

vertical movements to have taken place since the Miocene, although he considered the possibility of an older stage of lateral displacement. More recently it has been shown that strike-slip movements occurred along the AFZ during the Neocomian, when the AFZ was active as a structure of the magmatic arc (Naranjo *et al.* 1984, Thiele & Pincheira 1984, Hervé 1987b, Scheuber 1987). During later stages only vertical movements took place (Thiele & Pincheira 1984, Hervé 1987a, Naranjo 1987, Scheuber 1987). This can be seen on the satellite photograph (Fig. 5) where a drainage system (pre-late Miocene) is cut by the main branch of the AFZ (Salar del Carmen Fault). According to Hervé (1987a) these vertical movements took place between 5.5 and 19 Ma. This paper concentrates on the stage of wrenching along the AFZ represented by mylonitic rocks.

MYLONITIC ROCKS FROM THE ATACAMA FAULT ZONE

Two groups of ductilely deformed rocks can be observed (Figs.2–4).

(a) The rocks of one of these groups formed under middle amphibolite-facies conditions in Jurassic plutonic rocks (mainly diorites but also gabbros and tonalites) and volcanic rocks and Paleozoic greywackes. The plutonic rocks are part of the huge batholith that crops out in the southern part of the Mejillones Peninsula and south of Antofagasta. Its age ranges between 200 and 150 Ma (Diaz *et al.* 1985, Damm *et al.* 1986). The time of deformation may be inferred from the K–Ar age of 163 ± 14 Ma of newly crystallized syndeformational amphiboles in the sheared diorite (Table 1), as this dating system closed soon after crystallization of the amphibole. This age, however, is considered to be a maximum, as possible incorporation of excess radiogenic argon in the hornblendes must be taken into consideration. The mean age of biotite and sphene of 137 ± 12 Ma represents a minimum date for the deformation. In fact, except for the K–Ar hornblende system, the mineral dating systems of Table 1 give ages that postdate deformation, as their closure temperature is much lower than the prevailing temperature of amphibolite-facies conditions.

(b) The other group of ductilely deformed rocks developed in early Cretaceous plutonic rocks (mainly tonalites) under greenschist-facies conditions. K–Ar dating of the tonalites using biotite and amphiboles by Hervé *et al.* (1985) gave an age of 135–122 Ma. In the recent literature there are some indications that deformation also took place during the early Cretaceous. K–Ar whole rock dating of a mylonite south of Antofagasta (24°23'S, 70°27'W) gave an age of 139 ± 5–131 ± 5 Ma (Hervé 1987b). K–Ar dating of amphiboles in a mylonite from the AFZ east-northeast of Chañaral (26°17.9'S, 70°20.6'W) gave an age of 126 ± 10 Ma (Naranjo *et al.* 1984). The fission-track datings mentioned above also point to an early Cretaceous age of shear deformation.

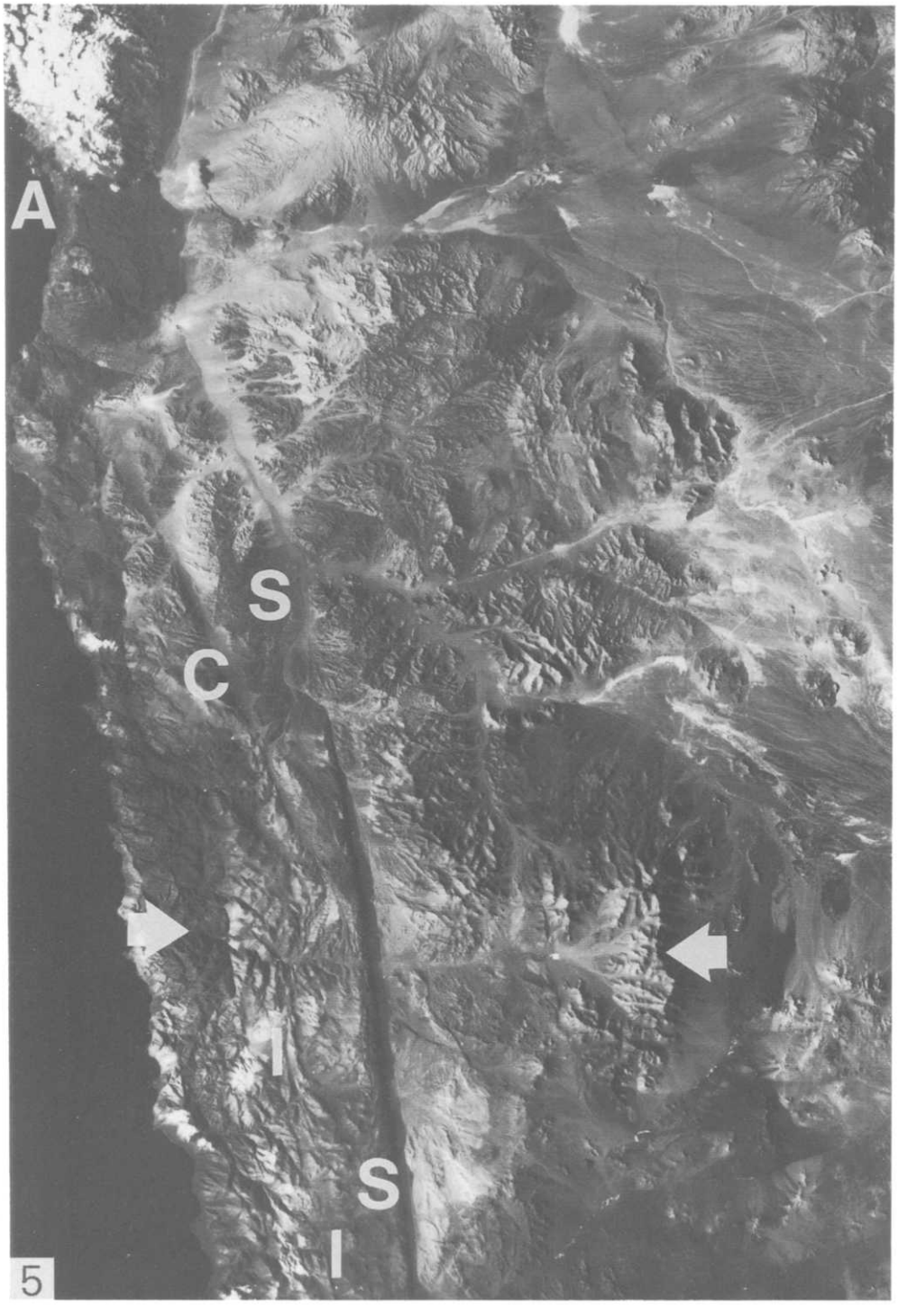

Fig. 5. MOMS (Modular Optoelectronic Multispectral Scanner) satellite image of the north Chilean Coastal Cordillera south of Antofagasta (A) (for location see Fig. 1). The AFZ, especially the Salar del Carmen Fault (main branch S) but also other branches (C: Coloso Fault, I: Izcuña Fault) are recognizable. In the lower half of the image a probable pre-late Miocene ESE–WNW-trending drainage system can be seen (indicated by arrows) cut by the Salar del Carmen Fault. The western block was uplifted with respect to the eastern, but evidently little lateral displacement took place.

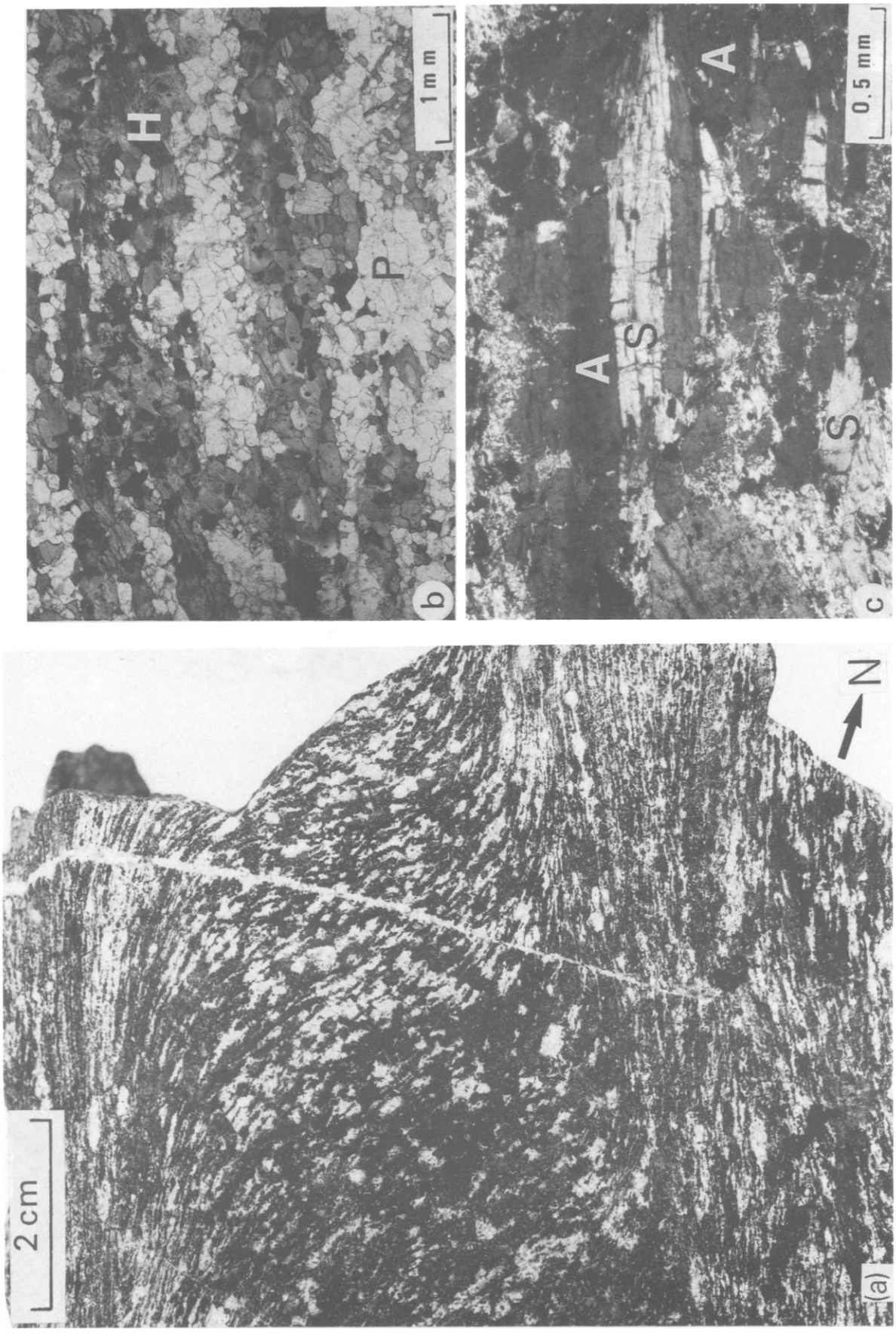

Fig. 6. The Jurassic shear zones. (a) Shear zones in a Jurassic diorite 37 km south of Antofagasta (Fig. 4). The vertically dipping mylonitic foliation bends asymptotically into the shear zones with a sinistral sense of shear. (b) Photomicrograph of the interior of one of these shear zones. Plagioclase (P) and hornblende (H) were completely dynamically recrystallized during shear deformation. (c) Sillimanite (S) and andalusite (A) in a paragneiss (2.8 km SE of Cerro Yumbes, Fig. 2).

Table 1. K–Ar and fission-track datings of sample Blf2b (sheared diorite from the Coastal Cordillera south of Antofagasta at 70°25′40″W/23°56′05″S. For location see Fig. 4)

Method	Mineral	Age (Ma)	Closure temp. (°C)	Reference
K–Ar	Hornblende	163 ± 14	490–580	(Harrison 1981)
K–Ar	Biotite	138 ± 9	300 ± 50	(Purdy & Jäger 1976)
Fission track	Sphene	136 ± 14	275 ± 50	(Gleadow & Lovering 1978)
Fission track	Zircon	119 ± 22	210–240	(Zaun & Wagner 1985, Hurford 1986)
Fission track	Apatite	118 ± 13	100 ± 20	(Wagner 1968, Naeser 1979)

Description of the mylonitic rocks

Jurassic shear zones. In numerous narrow N–S-trending shear zones of a few mm to 15 m width, foliated rocks developed, with transitions from mesoscopically isotropic Jurassic gabbros to tonalites. To a minor extent Jurassic volcanic rocks and Paleozoic greywackes are included in the shear zones. In some places the mylonitic foliation can be observed to bend into the shear zones (Fig. 6a). According to Nicolas & Poirier (1976), Ramsay (1980) and White *et al.* (1980), the mylonitic foliation represents the *XY* plane of the finite strain ellipsoid. The foliation contains the ± horizontal stretching lineation (the *X* direction) which is not fully developed throughout. The reason may be due to annealing, which can be inferred from post-deformational retrograde metamorphism that affected parts of the fabric in the sheared rocks (see below). In the mapped area of Fig. 2 the zone of sheared rocks is only some 500 m wide. It broadens towards the north and south of Antofagasta it reaches a width of 15 km and *ca* 10 km in the south of Mejillones Peninsula.

Except for some deflections, for example south of the Cerro Cristales (Fig. 4), the almost vertical mylonitic foliation trends NNE. Regarding the development of the mylonitic foliations west and southwest of the Cerro Cristales, Uribe & Niemeyer (1984) suggested a forceful emplacement of a pluton (plutón de Cerro Cristales) into Jurassic volcanics without any relation to the AFZ. However, according to the criteria for syntectonic diapirism of igneous bodies suggested by Bateman (1984), this can be excluded for most of the Jurassic shear zones. The reasons are: (i) the batholiths that suffered shear deformation are not circular or ovoid in plan but have rather irregular outlines; and (ii) the foliations do not form closed circular outlines close to the contact of the plutonic body but rather cut through the batholith and run subparallel to the trace of the AFZ.

Augen gneisses and amphibolitic gneisses formed from Jurassic igneous rocks. West-southwest of the Cerro Yumbes, Paleozoic greywackes also suffered shear deformation to produce paragneisses (see Fig. 2). The augen gneisses are light grey foliated rocks with porphyroclasts of igneous plagioclase (An_{30-40}), green hornblende (sometimes with clinopyroxene) and biotite surrounded by a ductilely deformed matrix of recrystallized quartz and plagioclase (An_{30-40}) and biotite. Quartz is generally absent in the dark-grey amphibolitic gneisses. Towards the interiors of the shear zones these rocks are strongly foliated and completely recrystallized with a mortar texture of plagioclase (An_{35-80}) and magnesio-hornblende with an average grain size of 0.1–0.3 mm (Fig. 6b). In the shear zone margins the content of igneous minerals of the gabbroic–dioritic protolith increases (igneous euhedral plagioclase, orthopyroxene, clinopyroxene, amphiboles). In contrast to the igneous minerals, the minerals recrystallized during shear deformation are always xenoblastic. A banding made up of alternating plagioclase-rich and amphibole-rich layers can frequently be observed. In some layers diopside is present. The paragneisses are fine-grained with lenticular banding of alternating metapsammitic layers rich in quartz and feldspar, and metapelitic layers rich in biotite and K-white mica. Cordierite, andalusite and sillimanite are present in most samples. Usually porphyroclasts do not occur in the paragneisses. Cordierite is almost completely pinitized. Sillimanite is idioblastic and never fibrolitic. In most cases it is surrounded by andalusite (Fig. 6c). Both minerals have straight low-energy mutual contacts and there is little evidence of replacement of sillimanite by andalusite. Due to the very small free energy for the reaction andalusite $\rightleftharpoons$ sillimanite, one phase may persist very easily into the stability field of the other (Brown & Fyfe 1971). The presence of both Al_2O_5 phases can thus be explained by metastable persistance of sillimanite into the stability field of andalusite. As both minerals are oriented parallel to the foliation they can both be considered as syntectonic.

The early Cretaceous shear zones. Together these shear zones are about 2 km wide, and their mylonitic rocks show a strong vertical foliation trending at an oblique angle to the AFZ trace (NNE–NE). The stretching lineation plunges 10–20° SSW–SW and is marked by the preferred orientation of amphibole- and plagioclase-porphyroclasts. Increasing ductile strain can be observed in a profile from the undeformed plutonic rocks to the interiors of the shear zones. The tonalites have a subhedral-granular texture of oligoclase + quartz + reddish-brown biotite + light green amphibole. Albite and K-feldspar are sometimes found. The original plutonic fabric without foliation is still well preserved on the margins of the shear zones. A mylonitic fabric develops towards the central parts of the shear zones, giving the rock a gneissic appearance. It is characterized by the contrast between a ductilely deformed quartz-rich matrix and brittle porphyroclasts of plagioclase and

amphibole. New syntectonically crystallized albite, actinolite, light brown biotite and/or chlorite, K-white mica and clinozoisite–epidote become abundant. Towards the central parts of the AFZ mylonitic zone ultramylonites may occur. They have less than 10% porphyroclasts and their matrix (intermediate plagioclase and quartz) is very fine grained.

ESTIMATIONS OF THE METAMORPHIC ENVIRONMENT

Metamorphic conditions during shear deformation were determined mainly with the help of syntectonic metamorphic minerals. Additional information was obtained from the chemical composition of amphiboles.

Jurassic shear zones

In the Jurassic shear zones metamorphic conditions during deformation are indicated by the following assemblages:

(1) In paragneisses:
andalusite + sillimanite + cordierite + K-white mica + biotite + quartz + intermediate plagioclase.

(2) In amphibolitic gneisses:
magnesio-hornblende or tschermakitic hornblende + intermediate to basic plagioclase ± diopside ± biotite ± sphene (quartz generally lacking).

Taking the Al_2O_5 triple point as determined by Holdaway (1971) (500°C, 380 MPa), which is generally accepted by field petrologists (Essene 1982), low-pressure conditions of the amphibolite-facies can be inferred from the presence of andalusite and sillimanite. Pressures <300 MPa are indicated by the presence of cordierite instead of almandine + staurolite (Richardson 1968). As there are no indications of the reaction muscovite + quartz = Al_2O_5 + K-feldspar + H_2O, temperatures could not have been much higher than about 600°C (if $P_{H_2O} = P_{total}$, Kerrick 1972). Temperatures within the amphibolite-facies are also indicated by the anorthite-content (>30%) of plagioclase (Wenk & Keller 1969) and the ductile behaviour of plagioclase which requires temperatures >500°C (White 1975, Tullis & Yund 1980).

The rocks of the Jurassic shear zones were strongly affected by a post-deformational retrograde metamorphism leading to the formation of biotite and K-white mica in paragneisses. Biotite, chlorite, K-white mica, epidote and prehnite formed in augen gneisses and amphibolitic gneisses. The post-deformational character of these minerals is indicated by the fact that they grew across the foliation without preferred orientation. Locally retrograde processes caused the tectonically acquired fabrics such as quartz *c*-axis preferred orientations and stretching lineations to become obscured.

Early Cretaceous shear zones

The tonalitic composition of the protolith of the early Cretaceous shear zones (quartz, oligiclase, green hornblende and biotite) is rather insensitive to significant changes in *P–T* conditions. Thus only a rough classification of the metamorphic grade in these rocks can be made. The minerals formed during deformation form the greenschist-facies assemblage

quartz + albite + actinolite + clinozoisite + biotite ± chlorite ± sphene.

The fact that quartz deformed ductilely whereas feldspar showed brittle behaviour also indicates greenschist-facies conditions (White 1975, Sibson 1977). The presence of biotite may point to temperatures >400°C (Winkler 1979).

Chemical composition of amphiboles

The chemical composition of amphiboles may change with increasing metamorphic grade (Binns 1965, Cooper & Lovering 1970, Raase 1974, Holland & Richardson 1979, Laird & Albee 1981, Hynes 1982, Laird *et al.* 1984, and others). However, rock composition also affects amphibole chemistry (Engel & Engel 1962) and may blur the *P–T* dependence. Generally, the variation in composition of metamorphic amphiboles that has been examined to a large extent concerns the Al^{IV}/Al^{VI} partitioning and the Na^A, Na(M4), Si and Ti contents.

Microprobe analyses were conducted with an ARL-SEMQ apparatus at 20 kV accelerating voltage and with 30 nA specimen current. All Fe was measured as FeO. A formula for amphiboles was calculated on the basis of 23 O (according to Robinson *et al.* 1982).

All measured amphiboles were recrystallized or newly crystallized during deformation. The diagrams (Figs. 7–9) indicate that they were formed under low-pressure–high-temperature conditions. This is consistent with the mineral assemblages of the paragneisses, and points to a high geothermal gradient (probably >50° km^{-1}) which is to be expected in the magmatic arc.

MICROSTRUCTURES AND QUARTZ *c*-AXIS FABRICS

Jurassic shear zones

The Jurassic shear zones show very different microstructures depending on the amount of quartz present. In quartz-free rocks plagioclase exhibits deformation bands, subgrains and new grains that indicate ductile behaviour (Fig. 6b). The progressive rotation of subgrains is regarded as the process of dynamic recrystallization during deformation of plagioclase (White 1975). Microstructures in quartz-rich rocks differ considerably, as quartz absorbs a large amount of the deformation. In most cases plagioclase porphyroclasts show only undulatory extinction and deformation bands, subgrains are

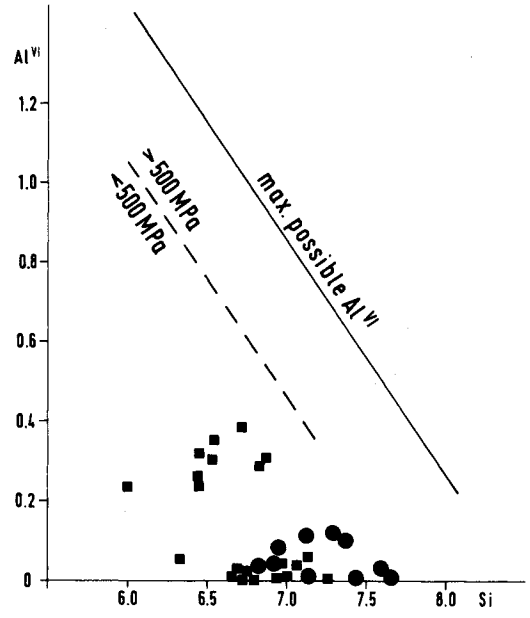

Fig. 7. Relation between Al^{VI} and Si in amphiboles from Jurassic (squares) and early Cretaceous (circles) mylonites between Antofagasta and Paposo (Fig. 4) (after Raase 1974).

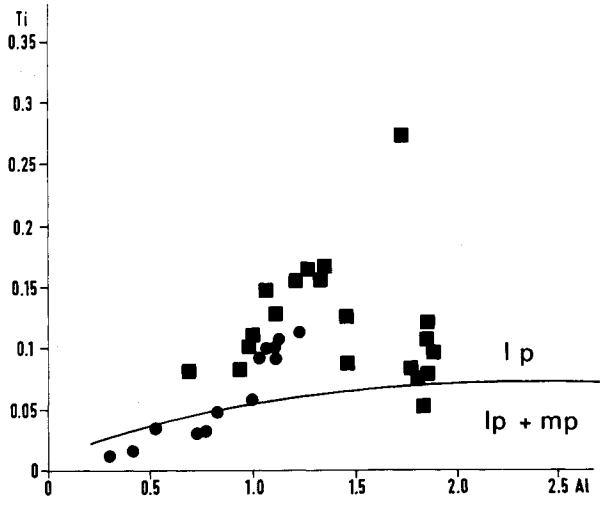

Fig. 9. Total Ti vs total Al (after Hynes 1982) of amphiboles (lp: the field of low-pressure amphiboles; lp + mp: the field of medium-pressure and low-pressure amphiboles) (symbols as in Fig. 7).

rare. Olsen & Kohlstedt (1985) attributed this to the higher dislocation density in quartz compared with that in plagioclase and thus to a much lower Peierl's stress in quartz than in plagioclase.

Quartz grains in Jurassic sheared rocks are elongated (long/short axis in *XZ* sections are 4 : 1 to 10 : 1). Grain boundaries are serrate to lobate, triple points (120°) and mortar textures are rare. The irregular shape of the quartz grains points to grain-boundary migration and pinning of boundaries by impurities (Gottstein & Mecking 1985). Bouchez & Pêcher (1981) described similar

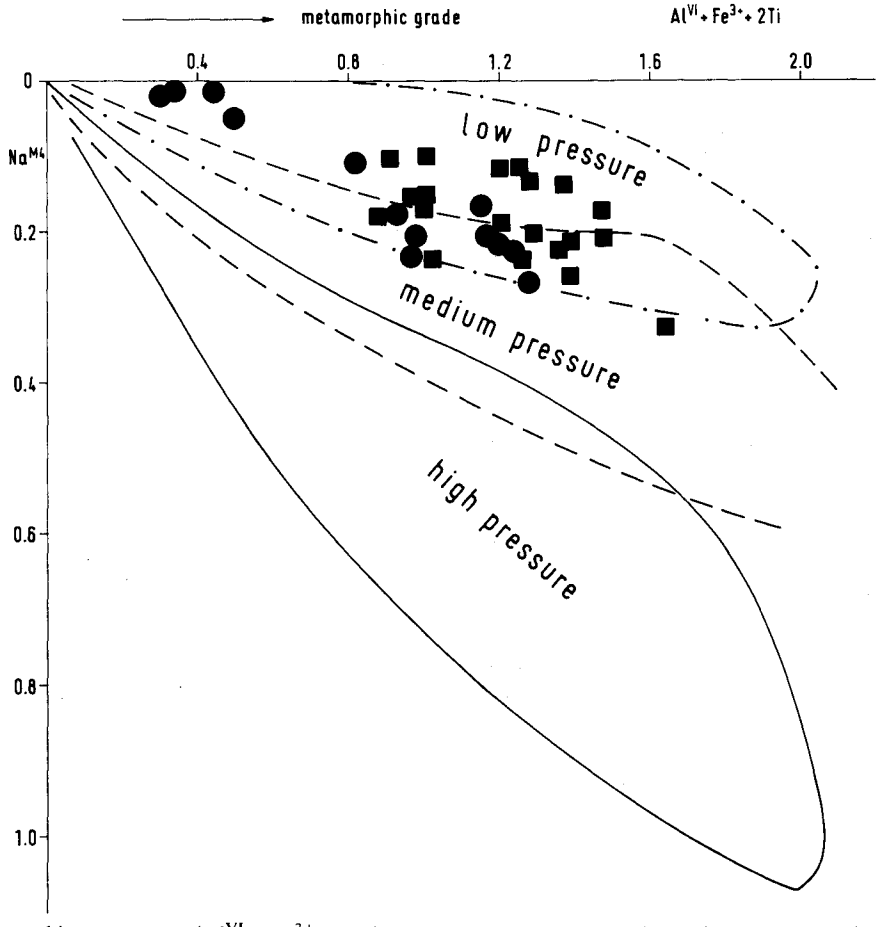

Fig. 8. Tschermakite component ($Al^{VI} + Fe^{3+} + 2Ti$) vs glaucophane component (NaM4) of amphiboles (after Laird *et al.* 1984, symbols as in Fig. 7).

quartz microstructures (grain-growth microstructures) from a high-grade terrain along the Himalayan Main Central Thrust. They put these structures down to post-tectonic exaggerated grain growth. This may also be the reason for the rather low degree of preferred orientation of quartz *c*-axes in the Jurassic shear zones along the AFZ. The quartz *c*-axis fabric skeletons of ortho- and paragneisses can be classified as type II crossed-girdles (Fig. 10) (Lister 1977) with an opening angle of 90–100°. Computer-simulations indicate that the theory that best explains the development of crossed-girdles is that of a combination of the basal-⟨*a*⟩, prism-⟨*a*⟩ and prism-⟨*c*⟩ glide systems during plane strain (Lister 1981). The opening angle of the crossed-girdles is possibly dependent on the relative ease of slip on the prism-⟨*c*⟩ glide system. The angle is small under low-grade metamorphic conditions (about 45°) and reaches a maximum of about 90° under high-grade conditions (Tullis *et al.* 1973, Blacic 1975, Behr 1980, Lister & Dornsiepen 1982). This is consistent with the amphibolite-facies deformation in the Jurassic shear zones. Type II crossed-girdles with one maximum around the intermediate strain axis *Y* suggest that the fabrics developed during plane strain (Tullis 1977) or under slightly constrictional conditions (Law 1986). This tallies with Lister's (1981) computer simulations. The symmetry of the skeletal outlines of the fabrics is orthorhombic, whereas the population within the skeletons is rather asymmetric. This may be explained by coaxial deformation paths in the closing stages of the deformation which may have obscured an older non-coaxial deformation history. A non-coaxial deformation history may be inferred from the fact that the 'sinistral' arms of the fabric skeletons are much more populated than the 'dextral' arms. As Lister & Williams (1979) pointed out, quartz *c*-axis fabrics are easily modified by a change in the deformation path, in which case the fabric skeleton may be symmetric (orthorhombic), although the arms are unevenly populated.

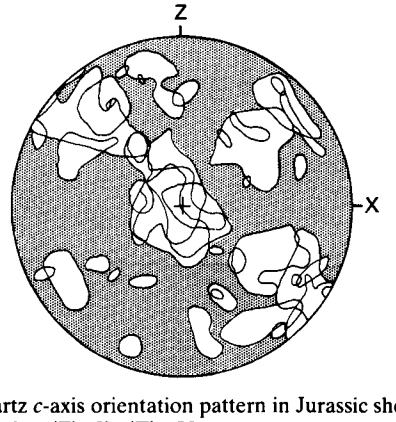

Fig. 10. Quartz *c*-axis orientation pattern in Jurassic shear zones SW of Cerro Yumbes (Fig.2). (The U-stage measurements were made in *XZ*-rock sections; this is a synoptic diagram of five diagrams containing all maxima with >2% measurements per 1% area; lower-hemisphere, equal-area projections, 1250 measurements.)

The early Cretaceous shear zones

The early Cretaceous mylonites show several microstructural features that indicate a non-coaxial deformation history. The quartz porphyroclasts are ribbon-shaped (long/short axis ratio in *XZ* sections ranging from 10 : 1 up to more than 25 : 1, in *YZ* sections around 1 : 5), and, to a lesser extent tabular (long/short axis 5 : 1–10 : 1). Globular quartz porphyroclasts that can be used as possible indicators of coaxial deformation paths (Law 1986) are generally absent. Elongate quartz subgrains are frequently obliquely oriented with a sinistral sense to the mylonitic foliation. As Burg (1986) pointed out, these obliquely oriented subgrains are reliable indicators of a non-coaxial deformation history.

The main foliation of the mylonites (the *S*-planes) is intersected by shear planes, the *C*-surfaces (Berthé *et al.* 1979) (Fig. 11a) which run subparallel to the shear zone margin. The angle θ between the two planes is large at the shear-zone boundary (about 40°) and decreases towards the interior of the shear zone. In the ultramylonites both surfaces almost coincide due to the exceptionally high strain in these rocks.

Ultramylonites from the central part of the AFZ show some very particular phenomena that indicate significant strains. The grain size of the plagioclase–quartz matrix depends on the flow stress or strain rate (White 1979) and is in most cases <2 μm (measured in thin sections). Evidence of very large strains in the ultramylonites is provided by apatite grains which were deformed to narrow bands, only 10–50 μm wide but longer than the whole thin section (2 cm, Fig. 11b), and also by diopside porphyroclasts stretched to string-of-pearl-like chains of small porphyroclasts also more than 2 cm long. Due to the large strain in the ultramylonites secondary extensional crenulation cleavages (*eccs*, Platt & Vissers 1980) developed (Fig. 11c). In contrast to *C*-planes, the *eccs* are not parallel with the shear-zone boundary.

In the mylonitic rocks quartz *c*-axes show good preferred orientations consistent with a non-coaxial deformation history (Fig. 13). They show oblique girdle patterns oriented perpendicular to the direction of shear. The absolute maxima of the quartz *c*-axis orientation patterns are situated in the vicinity of the intermediate strain axis *Y*; this is especially obvious in the very highly strained polycrystalline ribbon grains of ultramylonites. The maximum close to *Y* suggests that the main deformation mechanism was prism-⟨*a*⟩ slip associated with some rhomb-⟨*a*⟩ slip (Burg 1986). This result coincides with the observation that in *XZ* sections many quartz grains, especially the ribbon grains, have dark grey or black interference colours. According to Nicolas & Poirier (1976), prism-⟨*a*⟩ slip becomes important at high temperatures and low strain rates. This contrasts with the described mylonites where this slip system seems to be more active in samples with a high strain rate as indicated by the small grain size in these rocks. On the other hand, there is no evidence for elevated temperatures in these rocks.

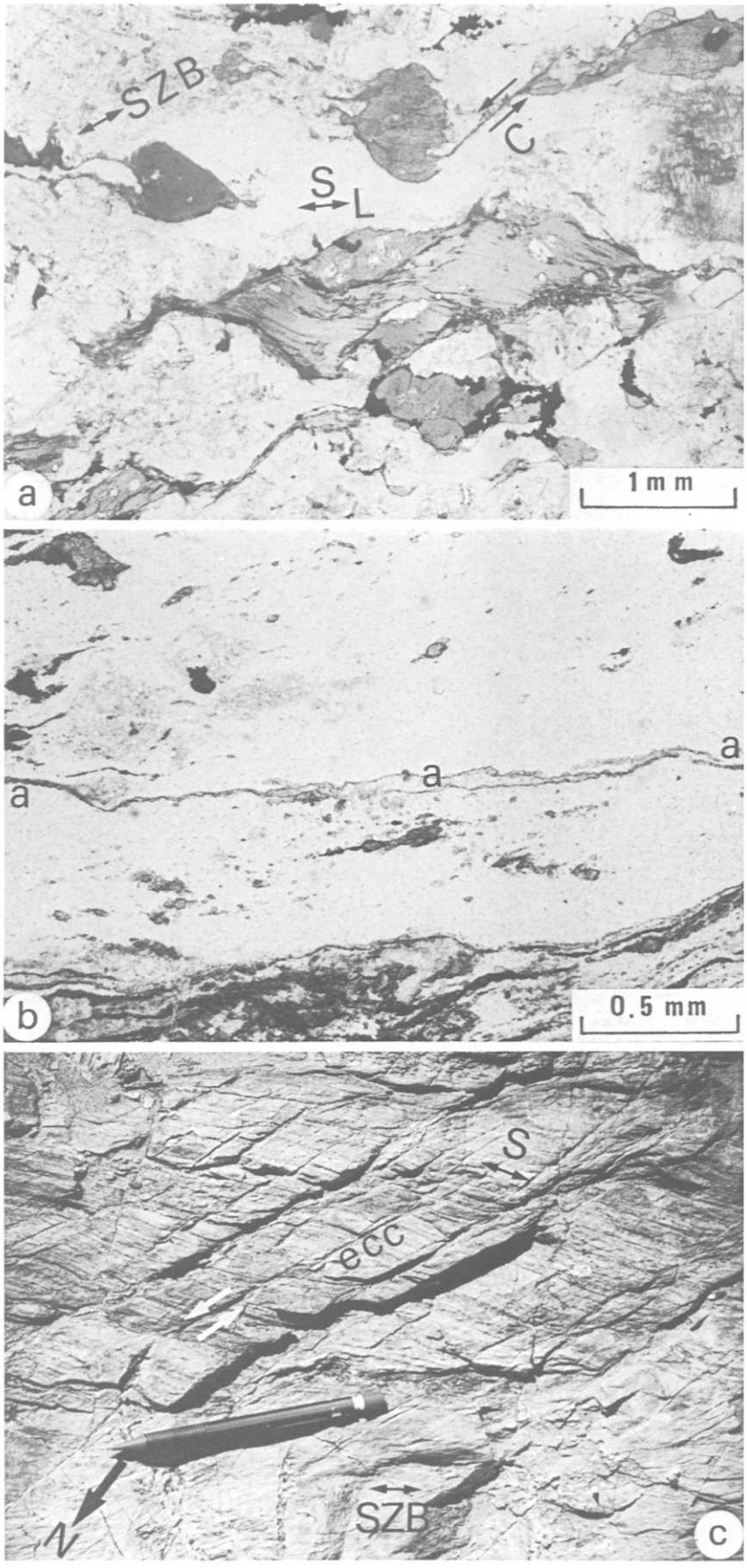

Fig. 11. Structural features in the early Cretaceous mylonites. (a) *S*- and *C*-planes in a tonalitic mylonite, 3.7 km east of Cerro Parañave (Fig. 2). Amphibole and biotite porphyroclasts are sheared along *C*-surfaces with sinistral sense. The *C*-surfaces run subparallel to the shear-zone boundary (SZB). The section is parallel to the horizontal stretching lineation (*L*). (b) Ultramylonite with an apatite ribbon (*a*) only a few μm wide but more than 2 cm long and indicating very intense strain within a *C*-plane. (From 6 km WSW of Cerro Paranal, Fig. 2.) (c) Extensional crenulation cleavage (*ecc*) in an intensely strained ultramylonite from the Quebrada Chañaral (Fig. 1). Mylonitic foliation (*S*) and *ecc*s dip vertically. SZB: direction of shear-zone boundary.

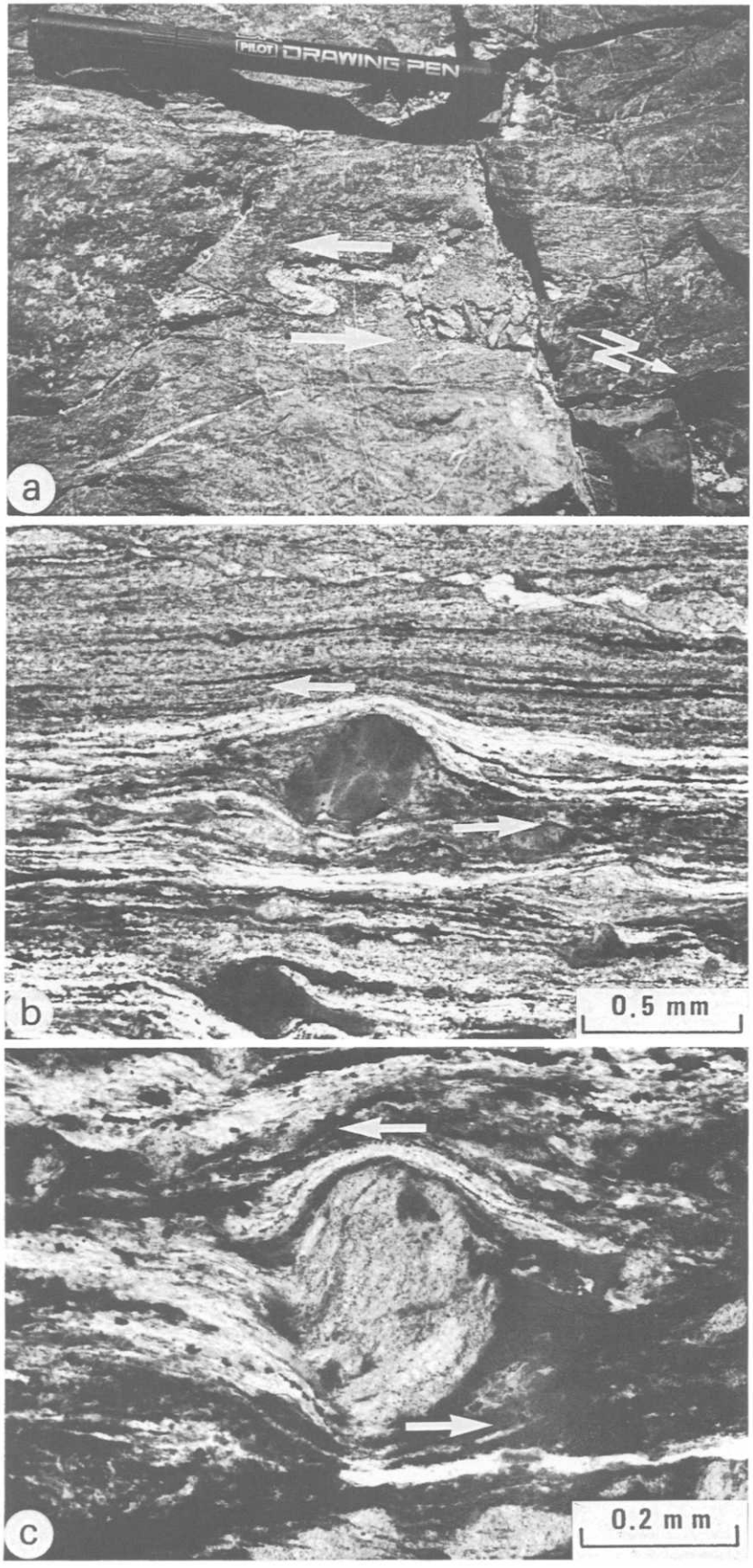

Fig. 12. (a) S-shaped isoclinal fold with vertical axis consistent with sinistral sense of shear in an amphibolitic gneiss (Jurassic shear zone 3 km SE of Cerro Yumbes, Fig. 2, with foliation dipping 299°/85°). (b) Non-rotated amphibole porphyroclast with asymmetric trains of recrystallized material (σ-porphyroclast according to Passchier & Simpson 1986). (c) Rotated albite, rolled in a sinistral sense (δ-porphyroclast). (b & c—XZ sections of an early Cretaceous ultramylonite from the Quebrada Chañaral, Fig. 1.)

STRUCTURAL ASYMMETRIES AND SENSE OF SHEAR

The sheared rocks along the AFZ exhibit an asymmetric pattern of structures on all scales that, according to Choukroune *et al.* (1987) indicates that bulk non-coaxial flow has occurred, and that the sense of shear is uniformly sinistral. On the macroscopic and mesoscopic scales the bending of the mylonitic foliation into the shear zones (Fig. 6a) indicates a sinistral sense of shear, as do the S-shaped folds with vertical axes (Fig. 12a) on the mesoscopic scale.

Statements about the sense of shear on the microscopic scale mainly concern the early Cretaceous mylonites. In the Jurassic shear zones post-deformational annealing has obscured most of these indicators. Only the unevenly populated quartz *c*-axis fabrics indicate that sinistral shearing occurred in these shear zones. In the early Cretaceous mylonites the following microstructural features indicate a sinistral sense of shear (according to the reviews of Simpson & Schmid 1983 and White *et al.* 1986).

(1) The mylonitic foliation is intersected by shear planes (*C*-planes, *eccs*), and is consistently bent into these shear planes with a sinistral sense (Figs. 11a & c).

(2) Brittle porphyroclast systems are very reliable indicators of the sense of shear. Both types, non-rotated ones (σ-porphyroclasts, Passchier & Simpson 1986) (Fig. 12b) and rotated ones (δ-porphyroclasts) (Fig. 12c) occur. Rotated porphyroclasts are restricted to highly strained mylonites and ultramylonites whereas non-rotated ones occur also in low-strain protomylonites. According to experiments by Passchier & Simpson (1986), δ-porphyroclasts occur when the recrystallization rate/strain rate ratio ($\dot{R}/\dot{\gamma}$) is low, whereas σ-porphyroclasts require higher $\dot{R}/\dot{\gamma}$ ratios.

(3) Elongate quartz subgrains and recrystallized grains are frequently oriented obliquely to the foliation plane. Such grains are interpreted by Brunel (1980) to be a consequence of dynamic recrystallization, and, as Burg (1986) demonstrated, this feature is a very reliable indicator of the sense of shear.

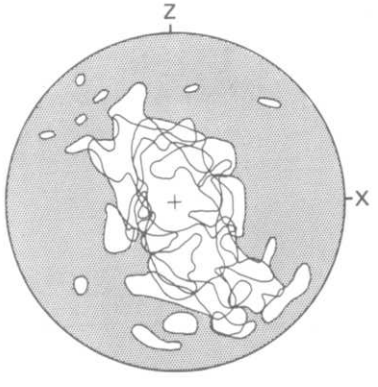

Fig. 13. Quartz *c*-axis orientation pattern in the early Cretaceous shear zones between 24°36′ and 24°49′S (Fig. 2). (The U-stage measurements were made in *XZ* rock sections; this is a synoptic diagram of five diagrams containing all maxima with >2% measurements per 1% area, lower-hemisphere, equal-area projection, 2000 measurements.)

(4) In the quartz *c*-axis fabrics of the mylonites, the left-sided asymmetry is uniformly and consistently developed and can thus be considered as a further indicator of the sense of shear.

As the sinistral sense of shear is developed uniformly in all samples over the whole area studied, one can assume that this is not a local effect but rather shows that bulk non-coaxial flow occurred along the AFZ and that the general sense of shear is sinistral.

DISCUSSION

The coincidence in time and space of wrenching along the AFZ with the Jurassic–early Cretaceous calc-alkaline magmatism (Fig. 1) allows a classification of the AFZ as a magmatic arc structure or as a trench-linked strike-slip fault *sensu* Woodcock (1986). The tectonics of the magmatic arc is a response by the crust of the upper plate to the forces generated by plate convergence. Crustal heating which can be inferred from the low-pressure–high-temperature conditions during shear deformation causes deformation to be focused on the magmatic arc. Differential stresses in magmas in a crust subject to deformation must be zero thus perturbating the regional stress field. Small amounts of melt reduce the strength of a rock drastically (e.g. Paquet *et al.* 1981). In the heated crust the brittle–ductile transition, which in quartz-rich rocks corresponds to the 300° isotherm (Sibson 1977), takes place at a higher level than it does under normal thermal conditions in the crust. Creep processes and the lack of strain hardening also gain significance in rather shallow crustal levels. A significant drop in differential stress and an increase in strain rate within the crust of the magmatic arc can thus be assumed. In addition, melts may function as lubricants in shear zones and increase deformation (Hollister & Crawford 1986). Once started, deformation in the magmatic arc is self-enhancing as at deeper crustal levels the significance of strain softening increases (White *et al.* 1980, 1986) due to grain refinement, accumulation of phyllosilicates in shear zones (reaction softening) and preferred orientation of lattices (geometrical or fabric softening).

CONCLUSIONS

The Jurassic–early Cretaceous period of wrenching along the AFZ can be interpreted as an intra-arc response to the forces acting at the plate boundary. If colliding plates move with a velocity vector at a much lower angle than 90° to the plate boundary (<60–70° according to Beck 1983), the vector is resolved into two components, one acting perpendicular to and one parallel to the plate boundary. Strike-slip movements due to oblique subduction were first described from Sumatra (Fitch 1972). Beck (1983) pointed out that factors that allow such 'Sunda-style' tectonics are a high angle of oblique convergence, a low angle of subduction dip and

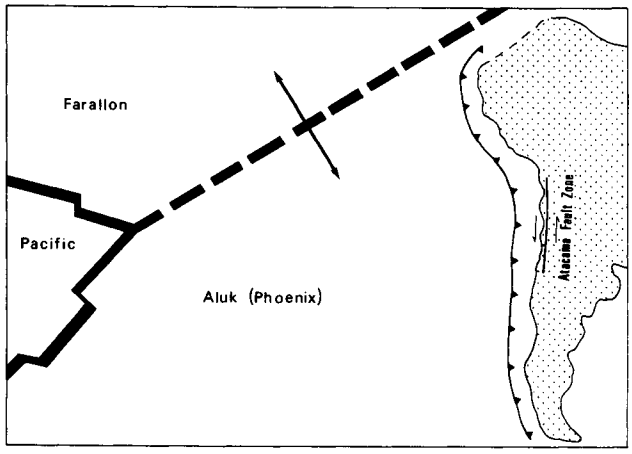

Fig. 14. Reconstruction of plate configurations and direction of spreading at the Jurassic–Cretaceous boundary (140 Ma), after Larson & Pitman (1972) and Zonenshayn *et al.* (1984).

a relative thermal softening in the magmatic arc by means of which the resistance to slip in a trench-parallel vertical zone in the arc is reduced compared with the inclined shear zone between the converging plates. The sense of shear in trench-linked strike-slip faults can help in reconstructing the direction of relative movement of the colliding plates. The sinistral sense of shear along the AFZ indicates that the oceanic plate moved in what today would be a SE direction. This coincides with the reconstruction of the plate configuration in the east Pacific in early Cretaceous times (Larson & Pitman 1972, Zonenshayn *et al.* 1984) (Fig. 14). The AFZ structures therefore support this kind of reconstruction.

As Woodcock (1986) has shown, the geometrical relation between the trench and the fault zone makes the possibility of it being a reactivated, old basement fault unlikely. On the other hand, trench-linked strike-slip faults are prone to later reactivation, due to the fact that they are preserved as zones of relative weakness (White *et al.* 1986). The AFZ was also reactivated as a steep normal fault after early Cretaceous times.

Acknowledgements—This work was part of the project "Mobility of Active Continental Margins" supported by the DFG (German Research Foundation). The K–Ar and fission track datings were supported by the Z.W.O. (Netherlands Organization for the Advancement of Pure Research). Special thanks to Prof. Dr A. Willgallis (Institut für Mineralogie, Freie Universität Berlin) for carrying out microprobe analyses. The DFVLR (German Research and Experimental Institute for Aviation and Space Technology) allowed publishing of the satellite image of Fig. 5.

REFERENCES

Arabasz, W. J. 1971. Geological and geophysical studies of the Atacama fault zone in northern Chile. Unpublished Ph.D. thesis, California Institute of Technology.

Bateman, R. 1984. On the role of diapirism in the segregation, ascent and final emplacement of granitoid magmas. *Tectonophysics* **110**, 211–231.

Beck, M. E. 1983. On the mechanism of tectonic transport in zones of oblique subduction. *Tectonophysics* **93**, 1–11.

Behr, H. J. 1980. Polyphase shear zones in the granulite belts along the margins of the Bohemian Massif. *J. Struct. Geol.* **2**, 249–254.

Berg, K. & Breikreuz, C. 1983. Mesozoische Plutone in der nordchilenischen Küstenkordillere: Petrogenese, Geochronologie, Geochemie und Geodynamik mantelbetonter Magmatite. *Geotekt. Forsch.* **66**, 1–107.

Berthé, D., Choukroune, P. & Jegouzo, P. 1979. Orthogneiss, mylonite and non coaxial deformation of granites: the example of the South Armorican Shear Zone. *J. Struct. Geol.* **1**, 31–42.

Binns, R. A. 1965. Hornblendes from some basic hornfelses in the New England region, New South Wales. *Mineralog. Mag.* **34**, 52–65.

Blacic, J. D. 1975. Plastic-deformation mechanisms in quartz: the effect of water. *Tectonophysics* **27**, 271—294.

Bouchez, J.-L. & Pêcher, A. 1981. The Himalayan Main Central Thrust pile and its quartz-rich tectonites in Central Nepal. *Tectonophysics* **78**, 23–50.

Brown, G. C. & Fyfe, W. S. 1971. Kyanite–andalusite equilibrium. *Contr. Miner. Petrol.* **33**, 227–231.

Brunel, M. 1980. Quartz fabrics in shear-zone mylonites: evidence for a major imprint due to late strain increments. *Tectonophysics* **64**, T33–T44.

Burg, J. P. 1986. Quartz shape fabric variations and *c*-axis fabrics in a ribbon-mylonite: arguments for an oscillating foliation. *J. Struct. Geol.* **8**, 123—131.

Choukroune, P., Gapais, D. & Merle, O. 1987. Shear criteria and structural symmetry. *J. Struct. Geol.* **9**, 525–530.

Coira, B., Davidson, J., Mpodozis, C. & Ramos, V. 1982. Tectonic and magmatic evolution of the Andes of northern Argentina and Chile. *Earth Sci. Rev.* **18**, 303–332.

Cooper, A. F. & Lovering, J. F. 1970. Greenschist amphiboles from Haast river, New Zealand. *Contr. Miner. Petrol.* **27**, 11–24.

Damm, K.-W. & Pichowiak, S. 1981. Geodynamik und Magmengenese in der Küstenkordillere Nordchiles zwischen Taltal und Chañaral. *Geotekt. Forsch.* **61**, 1–166.

Damm, K.-W., Pichowiak, S. & Todt, W. 1986. Geochemie, Petrologie und Geochronologie der Plutonite und des metamorphen Grundgebirges in Nordchile. *Berliner geowiss. Abh.* **A66**, 73–146.

Diaz, M., Cordani, U. G., Kawashita, K., Baeza, L., Venegas, R., Hervé, F. & Munizaga, F. 1985. Preliminary radiometric ages from the Mejillones Peninsula, Northern Chile. *Comunicaciones Univ. Santiago* **35**, 59–67.

Engel, A. E. J. & Engel, C. G. 1962. Hornblendes formed during progressive metamorphism of amphibolites, north-west Adirondack Mountains, New York. *Bull. geol. Soc. Am.* **73**, 1499–1515.

Essene, E. J. 1982. Geologic thermometry and barometry. In: *Characterization of Metamorphism Through Mineral Equilibria* (edited by Ferry, J. M.). *Miner. Soc. Am., Rev. Mineral.* **10**, 153–206.

Fitch, T. J. 1972. Plate convergence, transcurrent faults, and internal deformation adjacent to Southeast Asia and western Pacific. *J. geophys. Res.* **77**, 4432–4460.

Garcia, F. 1967. Geologia del Norte Grande de Chile. *Soc. Geol. Chile. Simposium sobre geosinclinal andina* 1962.

Gleadow, A. J. W. & Lovering, J. F. 1978. Thermal history of granitic rocks from Western Victoria: a fission track dating study. *J. geol. Soc. Aust.* **25**, 323–340.

Gottstein, G. & Mecking, H. 1985. Recrystallization. In: *Preferred Orientation in Deformed Metals and Rocks: An Introduction to Modern Texture Analysis* (edited by Wenk, H.-R.). Academic Press, Orlando, Florida, 183–218.

Gröschke, M., Hillebrandt, A. v., Prinz, P., Quinzio, L. A. & Wilke, H.-G. 1988. Marine Mesozoic Paleogeography in Northern Chile between 21° and 26°S. In: *The Southern Central Andes* (edited by Bahlburg, H., Breitkreuz, C. & Giese, P.). *Lecture Notes in Earth Sciences* **17**, 105–117.

Halpern, M. 1978. Geological significance of Rb-Sr isotopic data of northern Chile crystalline rocks of the Andean orogen between 23° and 27°S. *Bull. geol. Soc. Am.* **89**, 522–532.

Harrison, T. M. 1981. Diffusion of ^{40}Ar in hornblende. *Contr. Miner. Petrol.* **78**, 324–331.

Hervé, M. 1987a. Movimiento normal de la Zona de Falla Atacama, en el Mioceno, Chile. *Revta geol. Chile* **31**, 31–36.

Hervé, M. 1987b. Movimiento sinistral en el Cretacico Inferior de la Zona de Falla Atacama al Norte de Paposo (24°S), Chile. *Revta geol. Chile* **31**, 37–42.

Hervé, M., Marinovic, N., Mpodozis, C. & Perez de Arce, C. 1985. Geocronologia K–Ar de la Cordillera de la Costa entre los 24° y 25° latitud sur. Antecedentes prelimnares. *IV Congreso Geologico Chileno, Resumenes* **4.19**, 158.

Holdaway, M. J. 1971. Stability of andalusite and the aluminium silicate phase diagram. *Am. J. Sci.* **271**, 97–131.

Holland, T. J. B. & Richardson, S. W. 1979. Amphibole zonation in metabasites as a guide to the evolution of metamorphic conditions. *Contr. Miner. Petrol.* **70**, 143–148.

Hollister, L. S. & Crawford, M. L. 1986. Melt-enhanced deformation: a major tectonic process. *Geology* **14**, 558–561.

Hurford, A. J. 1986. Cooling and uplift patterns in the Lepontine Alps, South Central Switzerland and age of vertical movements on the Insubric fault line. *Contr. Miner. Petrol.* **92**, 413–427.

Hynes, A. 1982. A comparison of amphiboles from medium- and low-pressure metabasites. *Contr. Miner. Petrol.* **81**, 119–126.

Kerrick, D. M. 1972. Experimental determination of muscovite + quartz stability with $P_{H_2O} < P_{total}$. *Am. J. Sci.* **272**, 946–958.

Laird, J. & Albee, A. L. 1981. Pressure, temperature, and time indicators in mafic schists: their application to reconstructing the polymetamorphic history of Vermont. *Am. J. Sci.*, **281**, 127–175.

Laird, J., Lanphere, M. & Albee, A. 1984. Distribution of Ordovician and Devonian metamorphism in mafic and pelitic schists from northern Vermont. *Am. J. Sci.* **284**, 376–413.

Larson, R. L. & Pitman, W. C. III. 1972. World-wide correlation of Mesozoic magnetic anomalies, and its implications. *Bull. geol. Soc. Am.* **83**, 3645–3662.

Law, R. D. 1986. Relationships between strain and quartz crystallographic fabrics in the Roche Maurice quartzites of Plougastel, western Britanny. *J. Struct. Geol.* **8**, 493–515.

Lister, G. S. 1977. Crossed-girdle *c*-axis fabrics in quartzites plastically deformed by plane strain and progressive simple shear. *Tectonophysics* **39**, 51–54.

Lister, G. S. 1981. The effect of the basal-prism mechanism switch on fabric development during plastic deformation of quartzite. *J. Struct. Geol.* **3**, 67–75.

Lister, G. S. & Dornsiepen, U. F. 1982. Fabric transitions in the Saxony granulite terrain. *J. Struct. Geol.* **4**, 81–92.

Lister, G. S. & Williams, P. F. 1979. Fabric development in shear zones: theoretical controls and observed phenomena. *J. Struct. Geol.* **1**, 283–297.

McNutt, R., Crocket, J. H., Clark, A. H., Caelles, J. C., Farrar, E., Haynes, S. & Zentilli, M. 1975. Initial $^{87}Sr/^{86}Sr$ ratios of plutonic and volcanic rocks of the central Andes between latitudes 26° and 29°S. *Earth & Planet. Sci. Lett.* **27**, 305–333.

Naeser, C. W. 1979. Fission track dating and geological annealing of fission tracks. In: *Lectures in Isotope Geology* (edited by Jäger, E. & Hunziker, J. C.). Springer, New York, 154–169.

Naranjo, J. A. 1987. Interpretación de la actividad Cenozoica superior a lo largo de la Zona de Falla Atacama, norte de Chile. *Revta geol. Chile* **31**, 43–55.

Naranjo, J. A., Hervé, F., Prieto, X. & Munizaga, F. 1984. Actividad mecánica de la Falla Atacama al este de Chañaral: milonitización y plutonismo. *Comunicaciones Univ. Santiago* **34**, 57–66.

Nicolas, A. & Poirier, J. P. 1976. *Crystalline Plasticity and Solid State Flow in Metamorphic Rocks.* J. Wiley, London.

Olsen, T. S. & Kohlstedt, D. L. 1985. Natural deformation and recrystallization of some intermediate plagioclase feldspars. *Tectonophysics* **111**, 107–131.

Paquet, J., Francois, P. & Nedelec, A. 1981. Effect of partial melting on rock deformation: experimental and natural evidences on rocks of granitic compositions. *Tectonophysics* **78**, 545–565.

Passchier, C. W. & Simpson, C. 1986. Porphyroclast systems as kinematic indicators. *J. Struct. Geol.* **8**, 831–843.

Platt, J. P. & Vissers, R. L. M. 1980. Extensional structures in anisotropic rocks. *J. Struct. Geol.* **2**, 397–410.

Purdy, J. W. & Jäger, E. 1976. K–Ar ages on rock-forming minerals from the Central Alps. *Mem. Inst. Geol., Univ. Padova,* **XXX**, 1–31.

Raase, P. 1974. Al and Ti contents of hornblende, indicators of pressure and temperature of regional metamorphism. *Contr. Miner. Petrol.* **45**, 231–236.

Ramsay, J. G. 1980. Shear zone geometry: a review. *J. Struct. Geol.* **2**, 83–99.

Reutter, K.-J., Giese, P., Götze, H.-J., Scheuber, E., Schwab, K., Schwarz, G. & Wigger, P. 1988. Structures and crustal developments of the Central Andes between 21° and 25°S. In: *The Southern Central Andes* (edited by Bahlburg, H., Brietkreuz, C. & Giese, P.). *Lecture Notes in Earth Sciences* **17**, 231–261.

Reutter, K.-J. & Scheuber, E. 1988. Relation between tectonics and magmatism in the Andes of northern Chile and adjacent areas between 21° and 25°S. *V Congr. Geol. Chileno Actas* **1**, A345–A363.

Richardson, S. W. 1968. Staurolite stability in a part of the system Fe–Al–Si–O–H. *J. Petrol.* **9**, 467–488.

Robinson, P., Spear, F. S., Schumacher, J. C., Laird, J., Klein, C., Evans, B. W. & Doolan, B. L. 1982. Phase relations of metamorphic amphiboles: natural occurrence and theory. In: *Amphiboles: Petrology and Experimental Phase Relations* (edited by Veblen, D. R. & Ribbe, P. H.). *Miner. Soc. Am., Rev. Mineral.* **9B**, 1–228.

Rössling, R. 1987. Petrologie in einem tiefen Stockwerk des jurassischen magmatischen Bogens in der nordchilenischen Küstenkordillere südlich von Antofagasta. Unpublished Ph.D. thesis, Freie Universität, Berlin.

Rössling, R., Scheuber, E. & Reutter, K.-J. 1986. Strukturen und petrologische Einheiten der nordchilenischen Küstenkordillere zwischen Antofagasta und Paposo.–10. Geowissenschaftl. Lateinamerika-Kolloquium Berlin, 19.-21.11.1986. Kurzfassungen der Beiträge. *Berliner geowiss. Abh.* **A66**, 174–178.

Scheuber, E. 1987. Geologie der nordchilenischen Küstenkordillere zwischen 24°30′ und 25°S–unter besonderer Berücksichtigung duktiler Scherzonen im Bereich des Atacama-Störungssystems. Unpublished Ph.D. thesis, Freie Universität, Berlin.

Servicio Nacional de Geologia y Mineria. 1982. Mapa geológico de Chile 1 : 1,000,000, Santiago (Chile).

Sibson, R. H. 1977. Fault rocks and fault mechanisms. *J. geol. Soc. Lond.* **133**, 191–213.

Simpson, C. & Schmid, S. M. 1983. An evaluation of criteria to deduce the sense of movement in sheared rocks. *Bull. geol. Soc. Am.* **94**, 1281–1288.

St. Amand, P. & Allen, C. R. 1960. Strike-slip faulting in northern Chile (abs.). *Bull. geol. Soc. Am.* **71**, 8965.

Thiele, R. & Pincheira, M. 1984. Las Megafallas Los Colorados-Portezuelo Tatara y La Sosita-Huantamé, en la extensión sur de la Zona de Falla Atacama, al NW de Vallenar. *Comunicaciones Univ. Santiago* **34**, 67—70.

Tullis, J. 1977. Preferred orientation of quartz produced by slip during plane strain. *Tectonophysics* **39**, 87–102.

Tullis, J. & Yund, R. A. 1980. Hydrolytic weakening of experimentally deformed Westerly granite and Hale albite rock. *J. Struct. Geol.* **2**, 439–451.

Tullis, J., Christie, J. M. & Griggs, D. T. 1973. Microstructures and preferred orientations of experimentally deformed quartzites. *Bull. geol. Soc. Am.* **84**, 297–314.

Uribe, F. & Niemeyer, H. 1984. Franjas miloniticas en la Cordillera de la Costa de Antofagasta (Cuadrangulo Cerro Cristales, 24°00′–24°15′S) y la distribución del basamento Precambrico. *Revta Geol. Chile* **23**, 87–91.

Wagner, G. A. 1968. Fission track dating of apatites. *Earth & Planet. Sci. Lett.* **4**, 411–415.

Wenk, E. & Keller, F. 1969. Isograde in Amphibolitserien der Zentralalpen. *Schweiz. miner. petrogr. Mitt.* **49**, 157–198.

White, S. 1975. Tectonic deformation and recrystallization of oligoclase. *Contr. Miner. Petrol.* **50**, 287–304.

White, S. 1979. Grain and sub-grain size variations across a mylonite zone. *Contr. Miner. Petrol.* **70**, 193–202.

White, S. H., Bretan, P. G. & Rutter, E. H. 1986. Fault-zone reactivation: kinematics and mechanisms. *Phil. Trans. R. Soc. Lond.* **A317**, 81–97.

White, S. H., Burrows, S. E., Carreras, J., Shaw, N. D. & Humphreys, F. J. 1980. On mylonites in ductile shear zones. *J. Struct. Geol.* **2**, 175–187.

Winkler, H. G. F. 1979. *Petrogenesis of Metamorphic Rocks* (5th edn). Springer, New York.

Woodcock, N. H. 1986. The role of strike-slip fault systems at plate boundaries. *Phil. Trans. R. Soc. Lond.* **A317**, 13–29.

Zaun, P. E. & Wagner, G. A. 1985. Fission-track stability in zircons under geological conditions. *Nuclear Tracks* **10**, 303–307.

Zonenshayn, L. P., Savostin, L. A. & Sedov, A. P. 1984. Global paleogeodynamic reconstructions for the last 160 million years. *Geotectonics* **18**, 181–195.